# Discrimination of powdery mildew and yellow rust of winter wheat using high-resolution hyperspectra and imageries

Liang Dong[1], Liu Na[1], Zhang Dongyan[1,2], Zhao Jinling[1,2], Lin Fenfang[1,3], Huang Linsheng[1], Zhang Qing[1], Ding Yuwan[1]

(1. Anhui Engineering Laboratory of Agro-Ecological Big Data, Anhui University, Hefei 230601, China;
2. National Engineering Research Center for Information Technology in Agriculture, Beijing 100097, China;
3. School of Geography and Remote Sensing, Nanjing University of Information Science & Technology, Nanjing 210044, China)

**Abstract:** Disease stress is one of the main factors causing a reduction in wheat production and threatening food security. How to distinguish similar diseases accurately and diagnose disease severity scientifically is becoming a hot topic worldwide. The objective of this study is to discriminate powdery mildew and yellow rust of winter wheat, two common fungal diseases in the Chinese wheat-growing region. In the study, a high-resolution hyperspectral imaging system (ImSpector V10E) was utilized to capture spectral and imagery information of wheat leaves infected by two diseases. The dimensionality reduction of hyperspectral images was done by using principal component analysis (PCA), and with the density slice method, the recognition accuracy for the disease area at leaf level can be 97%. On this basis, the spectral difference of two diseases was analyzed, and 12 disease-sensitive bands were selected in the light of the second principal component (PC-2) images. The bands for powdery mildew were at 519, 643, 696, 764, 795 and 813 nm, while those for yellow rust were at 494, 630, 637, 698, 755 and 805 nm. Furthermore, a support vector machine (SVM) discriminant model was established based on selected sensitive wavebands, and its accuracy reached 92%. The results revealed that the hyperspectra combined with feature extraction of high-resolution imagery could effectively achieve discrimination of powdery mildew and yellow rust at leaf level, which will provide a theoretical foundation for developing a portable recognition device.

**Key words:** hyperspectra; principal component analysis; support vector machine; density slice; disease discrimination

**CLC number:** TP79; S127 **Document code:** A **DOI:** 10.3788/IRLA201746.0138004

# 利用成像高光谱区分冬小麦白粉病与条锈病

梁 栋[1],刘 娜[1],张东彦[1,2],赵晋陵[1,2],林芬芳[1,3],黄林生[1],张 庆[1],丁玉婉[1]

(1. 安徽省农业生态大数据工程实验室 安徽大学,安徽 合肥 230601;
2. 国家农业信息化工程技术研究中心,北京 100097;
3. 南京信息工程大学 地理与遥感学院,江苏 南京 210044)

**收稿日期**:2016-05-05; **修订日期**:2016-06-03

**基金项目**:国家自然科学基金(41301471,41301505);高等学校博士学科点专项科研基金新教师类(20133401120003);安徽省自然科学基金(1608085MF139);安徽省科技重大专项项目(16030701091)

**作者简介**:梁栋(1963-),男,教授,博士,主要从事计算机视觉技术应用方面的研究。Email:dliang@ahu.edu.cn

**通讯作者**:张东彦(1982-),男,副教授,博士,主要从事高光谱技术应用方面的研究。Email:hello-lion@hotmail.com

**摘 要**：病害胁迫是造成小麦减产及危及世界粮食安全的主要因素之一。如何准确区分相似病害并科学诊断病害严重度，成为国内外研究热点。文中针对中国冬小麦种植区常见的两种真菌疾病——白粉病和条锈病，采用高光谱成像系统获取两种病害侵染的小麦叶片图谱合一数据，通过主成分分析法对影像数据进行降维、密度分割法对病害面积进行分割后，得到识别病斑准确率达到 97%；进一步分析侵染白粉病和条锈病的叶片病斑区域的光谱特征差异，选择第二主成分图像筛选两种病害的敏感波段，得到识别白粉病的敏感波段为 519、643、696、764、795、813 nm，条锈病的敏感波段为 494、630、637、698、755、805 nm。最后对筛选出的敏感波段建立白粉病和条锈病支持向量机(SVM)判别模型并验证，得到两种病害的区分精度为 92%。综上，利用高光谱图像协同解析可在叶片尺度实现小麦白粉病和条锈病的有效判别，这为开发病害区分仪器提供了重要的理论基础。

**关键词**：高光谱； 主成分分析(PCA)； 支持向量机(SVM)； 密度分割； 病害判别

## 0 Introduction

Crop diseases and pests are primary obstacles to agricultural production that always affect crop yield and restrict sustainable agricultural development[1-2]. Traditional detection of crop diseases and pests adopts artificial experience due to the limitations of technology and production conditions. Lagged information seriously affects the forecasting accuracy for crop diseases and pests and can easily cause a loss of agricultural production. The surface feature spectrum data is based on the spectral characteristics of crops, ignoring the image features. Most of the non-imaging spectrometers obtain a combination of spectral data of leaf and canopy, which is vulnerable to the influence of the background. The high-resolution hyperspectral imagery has both spectral information and image information, providing reliable data for accurate analytical basis. High-resolution hyperspectral imagery has the advantages of providing both spectra and images and it can accurately find the occurrence and development of spatial distribution information of crop diseases and pests over a wide range. It can provide data support for agricultural decision-makers to take certain precautions to avoid damage to crops by diseases and pests[3-4]. At present, many scholars are applying this technique to diagnose crop diseases and pests. Hu et al. extracted disease spots on apple tree leaves using hyperspectral imagery, which provided method support for the remote sensing monitoring of crop diseases and pests[5]. Liu et al. found that reflectivity at around 550, 568, 605, 623, 660, 697, 715 and 733 nm were associated with wheat gibberellic disease[6]. Yang and Cheng analyzed a rice canopy infected with brown planthopper and revealed that the reflectivity of 737-925 nm responded better to disease infection[7]. Zhang et al. pointed out that hyperspectral imaging technology provides unique advantages in the quantitative and qualitative analysis of crop growth through analyzing hyperspectra and images of wheat leaves under different stresses[8].

Powdery mildew and yellow rust are two common diseases of winter wheat in China. Preventing and managing them is a great challenge because of the coincidence of their occurrence in the field[9]. From works reported in the literature, we found that present studies are focused on a specific kind of the disease. Feng et al. showed that the reflectance at 350-710 nm increased with the disease severity of powdery mildew, and 580-710 nm was selected as the sensitive waveband for monitoring[10]. Huang et al. explored the relationship between spectra and the disease index of wheat yellow rust, and pointed out that 630-687, 740-890, and 976-1350 nm were sensitive wavebands for the detection of yellow rust[11]. By summarizing the above studies, we found that the sensitive wavebands of the two diseases had similar range intervals and different bands at leaf and canopy

level. The two diseases has similarity, because they are affected by the change of pigment content, which impacts on photosynthesis and leads to the spectral similarity in the corresponding chlorophyll content region; the differences are mainly caused by the different varieties, growth periods, and so on, which create changes of shape and structure in wheat plants at canopy and leaf level and lead to the spectral differences. Currently, there are few studies focused on comparing the spectral response to powdery mildew and yellow rust. Generally, the two diseases can occur at the same growth stage in the field, and thus it is necessary to spray different fungicides to prevent them. So it is very necessary to distinguish the spectral features of the two diseases and also to guide the field production arrangement. However, our research group has preliminarily found that the spectra at around 490−532, 665−684, 718−726, 737−1 000, and 1 368−1 376 nm could distinguish the two diseases using correlation analysis and independent $T$−test, and a discriminant model with more than 80% accuracy was set up[12]. The spectral sensor has only dot-shaped spectral data, and potential artificial operation errors due to different technicians probably affect the accuracy of discrimination of disease characteristics. Thus the use of new sensors and technology to identify the two diseases is indispensable.

In this study, high-resolution hyperspectral images of wheat powdery mildew and yellow rust were collected. We utilized the method of image segmentation and spectral identification to: (1) determine the main components of the images suitable for segmentation of healthy and diseased areas using principal component analysis (PCA); (2) recognize the diseased areas of two types using the density slice method and analyzed the differences in the spectral response to wheat yellow rust and powdery mildew at leaf level; (3) established a spectral discriminant model of the two diseases. The aim is to provide the theoretical basis for developing a device for the automatic identification of the two diseases.

## 1 Materials and methods

### 1.1 Experimental design

In this experiment, the wheat varieties "Jing 9843" and "JingShuang 16", which are susceptible to yellow rust and powdery mildew, respectively, were chosen as research samples. In early October, 2012, the winter wheat was sowed at the experimental farm of Beijing Academy of Agriculture and Forestry Sciences under conventional field management. In early March, 2013, the healthy winter wheat plants were artificially sprayed with fungal liquid[10]. When the wheat had grown to the filling stage, the healthy and disease-infected leaves were picked and preserved in a portable cold closet in the field. Then high-resolution hyperspectral images were captured in the laboratory. To the test of wheat yellow rust, a total of 83 leaves (26 healthy leaves, 57 infected leaves) were selected, To the test of wheat powdery mildew, a total of 92 leaves (26 healthy leaves, 66 infected leaves) were selected.

### 1.2 Hyperspectral imaging system

An ImSpector V10E hyperspectral imaging spectrometer (Fig.1) was used in this study to collect

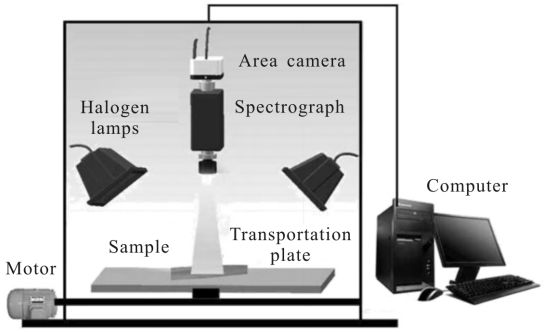


Fig.1 Hyperspectral image acquisition platform

image and spectral data[13]. It was noted that the spectral resolution of the V10E instrument was higher than that of the ASD instrument and that the V10E could obtain high-resolution hyperspectral images, reaching a unity of the spectrum and image[13]. This is helpful for analyzing disease characteristics at both micro-dot and

leaf level accurately and has advantages for the disease feature extraction. Although the ASD instrument has a wider spectral range and is commonly used in agricultural analysis, the shortage of a non-imaging spectrum often leads to certain research errors [8]. In particular, the measurement accuracy is easily affected by different operating personnel.

Images of wheat powdery mildew and yellow rust within the wavelength range of 400-1 000 nm acquired by the platform are shown in Fig.2. The size of the images was 1 000 mm×570 mm. An image of the leaves infected with powdery mildew is shown in Fig.2(a). Figure 2 (b) shows leaves with yellow rust along with three leaves on the right side that are healthy.

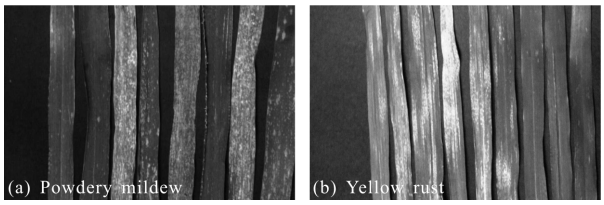


Fig.2 False images of powdery mildew (a) and yellow rust (b) at 453(R), 313(G), and 173(B) nm

### 1.3 Data analysis and processing

The technology flow chart is shown in Fig.3. In this study, data analysis and processing included: (1) the segmentation of diseased and healthy areas; (2) the spectral standardization of the two diseases; (3) extraction of bands that are sensitive to the two diseases; (4) establishment of the spectral discriminant model of the two diseases.

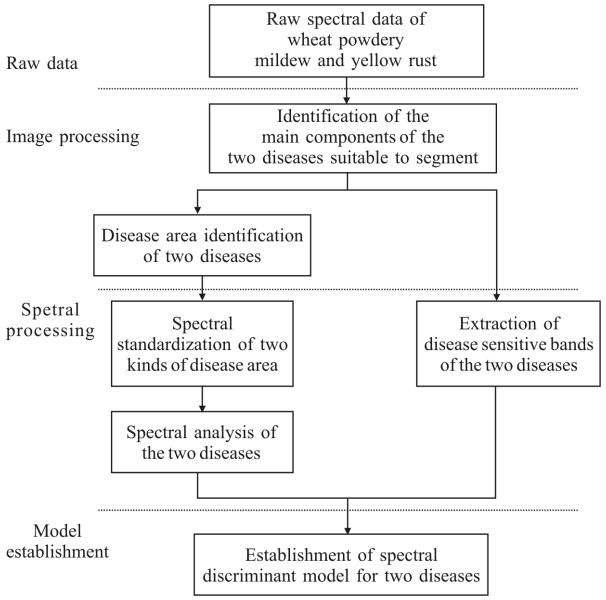


Fig.3 Technology flow chart

#### 1.3.1 Principal component analysis of high-resolution images

By analyzing the wavebands with the most useful information, we can simplify the data to establish the discriminant model of the two diseases [4]. Principal component analysis (PCA) was utilized to compress the spatial-spectral dimensionality of the hyperspectral image. Each principal component (PC) image is a linear sum of the original images at individual wavelengths multiplied by corresponding weighted coefficients [14]. This method is a multi-band linear variation which transforms the data into a new coordinate system in order to maximize the data differences. Since each PC image is made by a linear combination of each band in the original data, we can select the best characteristics of the image through the selection of the weighting coefficient of the linear combination [14]. In this study, the first five PC images are able to reveal the main features of the two leaf diseases. The cumulative contribution rate that the first five principal components contains has reached 97.89%, it shows that the first five principal components can explain 97.89 percent of the information in the original spectral data(see Tab.1). All of the images are illustrated in Fig.4. Through visual inspection, we found that the PC-1 image contained the most original information and PC-5 was mostly filled with noise. The diseased areas appeared slightly in PC-1 and noise appeared in PC-3, PC-4, and PC-5, causing relatively low contrast between the diseased and healthy areas. Thus, the PC-2 image provides the most potential for identifying the diseased area of fungus-infected leaves, and therefore it was chosen for extracting the characteristic wavebands.

**Tab.1 Cumulative contribution rate of five principle components**

| No. of PC | PC1 | PC2 | PC3 | PC4 | PC5 |
|---|---|---|---|---|---|
| Percent | −75.87% | 86.32% | −92.15% | −97.62% | 97.89% |

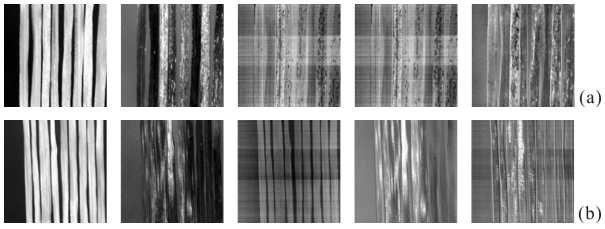

Fig.4 Images of PC−1, PC−2, PC−3, PC−4, and PC−5 of powdery mildew (a) and yellow rust (b)

1.3.2 Image segmentation

A hyperspectral image of leaves contains two-dimensional information[8], and thus in this study image segmentation is a necessary procedure to effectively identify and extract the disease spots. It is an image-processing technology that divides the image into a number of meaningful areas as required[15]. The dimensions of the original hyperspectral images were greatly reduced using principal component analysis. At the same time, most of the image information was compressed and concentrated in the former main components of the image[16]. Density segmentation was used to explain the second principal component image (PC−2) of the two diseases. The method is commonly used to extract the information characteristics of remote sensing images and is similar to the multilevel threshold method; namely it selects a dividing point according to the image′s gray value and probability distribution [17]. The gray value can be divided into several levels, representing different ownership types. Because the average gray value of diseased spots was lower than that of the healthy areas in the two PC−2 images, we divided the gray values into two levels according to the distribution characteristics of the gray value. One kind was diseased spots, and the other kind was healthy areas. The diseased spots of wheat powdery mildew and yellow rust were extracted by segmenting different gray values in order to realize the separation of diseased spots and healthy parts.

1.3.3 Spectral normalization

To reduce the impact on the spectral data of powdery mildew and yellow rust caused by the differences in varieties and with time, it is essential to normalize the spectral data before carrying out the comparative analysis. We referenced the spectral standardization method of the literature to control the influence and obtain better results[12].

First of all, we defined $A$ as the spectral mean of powdery mildew healthy leaves, and $B$ as the spectral mean of yellow rust healthy leaves, then calculated the ratio of $A$ to $B$. The formula is as follows:

$$\mathrm{Ratio}_i=\frac{\overline{\mathrm{Ref}_{(\mathrm{PM})_i}}}{\overline{\mathrm{Ref}_{(\mathrm{YR})_i}}} \tag{1}$$

where $i$ is the waveband, Ref is reflectance, and subscripts YR and PM are yellow rust and powdery mildew, respectively. Secondly, this ratio value was multiplied by every spectrum of yellow rust samples collected, and then we could obtain the normalized spectral data of yellow rust. The normalization formula for a waveband is:

$$\mathrm{Ref}'_{(\mathrm{YR})_i}=\mathrm{Ref}_{(\mathrm{YR})_i}\times\mathrm{Ratio}_i \tag{2}$$

where $\mathrm{Ref}_{(\mathrm{YR})_i}$ is the primary spectral reflectance of band $i$ of yellow rust, and $\mathrm{Ref}'_{(\mathrm{YR})_i}$ is the reflectance after normalization. The above normalization calculation could not change the relative spectral differences between healthy and diseased leaves and only modified every spectrum of yellow rust using the same ratio value. The same procedure was also used to normalize the reflectance of powdery mildew. Finally we tried to exclude the negative influences on the spectral analysis caused by the differences in varieties and duration of the two diseases and also improved the reliability in distinguishing the two types of spectral data.

1.3.4 Discriminant model establishment

On the above basis, Support Vector Machine (SVM) was selected to construct a discriminant model

of the two diseases because it can not only minimize the sampling error but also reduce the structural risk. Meanwhile, this method improves the generalization ability of the model, and there is no limit on the data dimension. In addition, the basic idea of SVM is to map the sample space to a high-dimensional or even infinite-dimensional feature space, realizing linear classification or regression through a linear hyperplane in the high-dimensional feature space[18]. This method could solve the problems of a small sample, nonlinearity, and high dimensionality, and moreover, it could overcome the local minima problem in the neural network. In this study, we chose the Radial Basis Function (RBF) as the kernel function.

## 2 Results and analysis

The binary images after image segmentation are shown as Fig.5. A total of 120 samples, comprising

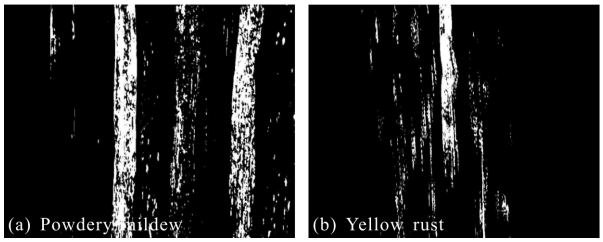


Fig.5 Binary images of powdery mildew (a) and yellow rust (b)

60 powdery mildew and 60 yellow rust samples, were analyzed. The results revealed that 58 powdery mildew samples and all yellow rust samples can be segmented fairly well, with an accuracy of more than 97% . The white parts of the images show the diseased areas (Fig.5). It was observed that we could distinguish the healthy and diseased areas according to the binary image distinctly and rapidly. Based on the binary images of powdery mildew and yellow rust, we selected the diseased spots as regions of interest(ROI) to extract their reflectance curves. Spectral analysis was carried out after standardizing the leaf spectra of wheat powdery mildew and yellow rust. As can be seen from Fig.6, the spectral reflectance of the two diseases at around 700−780 nm had similar responses, and the spectral reflectance at around 550−700 nm revealed the largest difference. The results of this study were basically identical to the results of Zhang et al [19]. Infection of mesophyll cells by bacteria could cause damage to the chloroplast structure and loss of cell moisture, leading to changes in the spectral reflectance at visible wavelengths and short-infrared wavelengths. In addition, as we can see in Fig.6, the spectral reflectance of the two diseases at around 420−550 nm had a larger difference. These wavebands primarily correspond to the chlorophyll content and cell structure. The leaf water content and leaf pigment content differ when leaves are infected by germs, leading to the formation of differently colored disease spots, resulting in different spectral reflectance. The above differences of spectral reflectance could be regarded as the basis for distinguishing the two diseases.

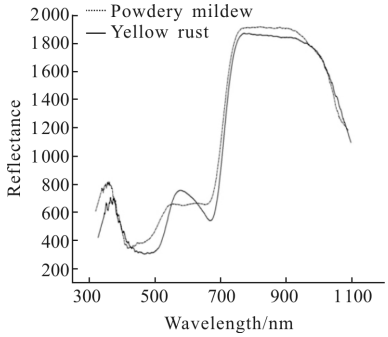


Fig.6 Hyperspectral curves of powdery mildew and yellow rust

The PC−2 images of the two diseases provided the most potential for differentiating disease features and were chosen for selecting the sensitive wavebands. The weighting coefficients of PC−2 images of the two diseases are displayed shown in Fig.7. The peaks and valleys in the weighting coefficients indicate the dominant wavebands. The sensitive bands of powdery mildew are at 519, 643, 696, 764, 795, and 813 nm (Fig.6 (a)) and those of yellow rust are at 494, 630, 637, 698, 755, and 805 nm(Fig.6(b)). It is imperative to select a proper method of calibration for spectral analysis, and thus PCA−SVM was utilized to establish the discriminant model of powdery mildew and yellow

rust. In this study, the PCA-SVM classifier was binary: the classifier code of powdery mildew was 0 and that of yellow rust was 1. Six disease-sensitive bands of powdery mildew and six of yellow rust were extracted and the twelve characteristic bands were selected to differentiate the two diseases. Yuan et al.

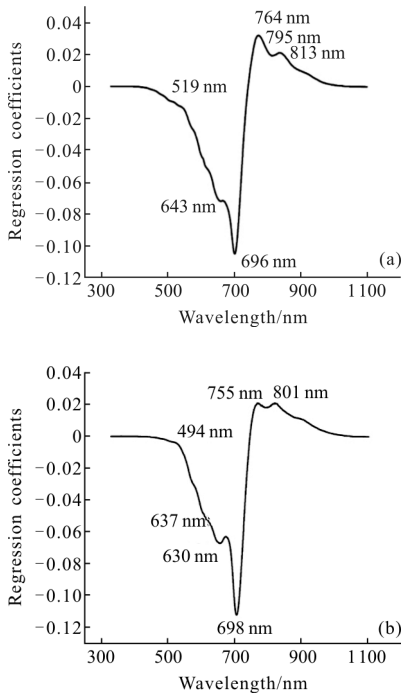


Fig.7 Weighting coefficients of powdery mildew (a) and yellow rust (b) based on the PC-2 image

(2013) indicated that the spectral features at around 490-532, 665-684, 718-726, 737-1 000, 1 368-1 376, and 1 891-2 014 nm could discriminate powdery mildew and yellow rust explicitly [12]. The wavebands selected in this study, at 494, 519, 755, 764, 795, 801, and 813 nm, are located in the ranges of Yuan's results. According to the construction of the normalized difference vegetation index (NDVI) [12], spectral regions of red and near-infrared were considered as the two band ranges that were sensitive to changes in the amount of green biomass and chlorophyll content. The wavebands at 630, 637, and 643 nm are located in the red spectral region and those at 696 and 698 nm are in the near-infrared region, so the twelve wavebands we selected to differentiate the two diseases were reliable. Accordingly, the reflectance located at 494, 630, 637, 698, 755, 805, 519, 643, 696, 764, 795, and 813 nm for powdery mildew and yellow rust were set as the independent variables and class codes were set as dependent variables for constructing the discrimination model. The penalty factor $C$ was set as 0.25 and $G$ was 1.148 7, and then 100 samples were selected as the training set and 50 samples as the testing set. We obtained a prediction accuracy of 92% (46/50). Only two yellow rust samples and powdery mildew samples were misjudged. The performance results of the discriminant model are illustrated shown in Fig.8.

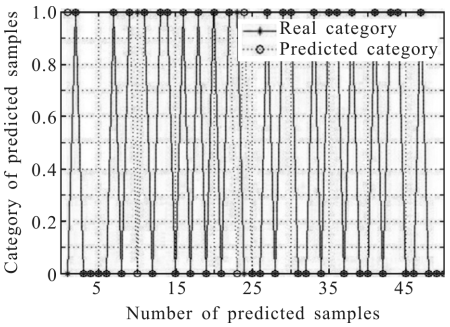


Fig.8 Results of the discrimination model

## 3 Conclusions and discussion

Powdery mildew and yellow rust are two significant diseases of winter wheat in China and have an enormous impact on the grain harvest. In this study, the hyperspectra combined with image features were utilized to discriminate powdery mildew and yellow rust. Principal Component Analysis (PCA) was used to identify the main components of the two diseases suitable for segmentation. The PC-2 images of the two diseases were chosen for segmenting the image and selecting characteristic wavebands. The density slice was used to distinguish the diseased and healthy areas, and its recognition accuracy reached 97%. On this basis, sensitive wavebands of powdery mildew at 519, 643, 696, 764, 795, and 813 nm were extracted as well as those of yellow rust at 494, 630, 637, 698, 755, and 805 nm. The PCA-SVM discriminant

model was established based on 12 disease-sensitive wavebands, which yielded a prediction accuracy of 92%. This study achieved the aim of discriminating and monitoring the two diseases at leaf level.

A valuable result is that the identification accuracy obtained in this study was higher than that obtained by other literature using non-imaging spectrometry [12]. It has been proven that hyperspectra combined with high-resolution imagery features are useful for improving the discrimination of similar wheat diseases, because the technology can extract the diseased area exactly at leaf level and then obtain the corresponding reflectance spectrum whose maximum avoids the effects of artificial operation on the accuracy of disease recognition. However, wheat disease features are often influenced significantly by complicated factors, especially in the occurrence of powdery mildew and yellow rust. Not only are changes of physiological and biochemical components displayed in different varieties, but also the environment has an important effect, because the same species shows differences in different growth years. All of these factors pose challenges to the accurate diagnosis of wheat diseases. Thus, further research will be focused on distinguishing the disease characteristics of multiple varieties and different growth periods, with the aim of obtaining stable identification accuracy of wheat diseases and providing effective data support for the development of a disease identification device.

## References:

[1] Chen Bing, Li Shaokun, Wang Kerv. Studies of remote sensing on monitoring crop diseases and pests [J]. ***Cotton Science***, 2007, 19(1): 57-63. (in Chinese)

[2] Chen Pengcheng, Zhang JianHua, Lei Yonghui. Research progress on hyperspectral remote sensing in monitoring crop diseases and insect pests [J]. ***Chinese Agricultural Science Bulletin***, 2006, 22(3):388-391. (in Chinese)

[3] Luo Hongxia, Kan Yingbo, Wang Lingling. Hyperspectral remote sensing for crop diseases and pest dectection [J]. ***Guangdong Agricultural Sciences***, 2012, 39(18): 76-80. (in Chinese)

[4] Zhang B H, Huang W, Li J B, et al. Principles, developments and applications of computer vision for external quality inspection of fruits and vegetables: A review [J]. ***Food Research International***, 2014, 62: 326-343.

[5] Hu Rongmeng, Wei Man. Research for extracting method of apple leaf ill spots based on hyperspectral image[J]. ***Journal of Northwest Agriculture and Forestry University (Natural Science Edition)***, 2012(8): 95-99. (in Chinese)

[6] Liu Liangyun, Huang Muyi, Huang Wenjiang. Monitoring stripe rust disease of winter wheat using muti-temporal hyperspectral airborne data [J]. ***Journal of Remote Sensing***, 2004, 8(3): 275-281.

[7] Yang C M, Cheng C H. Spectral characteristics of rice plants infested by brown planthoppers [J]. ***Proceedings of the National Science Council Republic of China Part B: Life Sciences***, 2001, 25(3): 180-186.

[8] Zhang Dongyan, Zhang Jingcheng, Zhu Dazhou, et al. Investigation of the hyperspectral image characteristics of wheat leaves under different stress [J]. ***Spectroscopy and Spectral Analysis***, 2011, 31(4): 1011-1105. (in Chinese)

[9] Kuckenberg J, Kuckenberg J, Tartachnyk I, et al. Detection and differentiation of nitrogen-deficiency, powdery mildew and leaf rust at wheat leaf and canopy level by laser-induced chlorophyll fluorescence [J]. ***Biosystem Engineering***, 2009, 103(2): 121-128.

[10] Feng Wei, Wang Xiaoyu, Song Xiao, et al. Estimation of severity level of wheat powdery mildew based on canopy spectral reflectance [J]. ***Acta Agronomica Sinica***, 2013, 39 (8): 1469-1477. (in Chinese)

[11] Huang Muyi, Wang Jihua, Huang Wenjiang. Hyperspectral character of stripe rust on winter wheat and monitoring by remote sensing [J]. ***Transactions of the CSAE***, 2003, 19(6): 154-158. (in Chinese)

[12] Yuan Lin, Zhang Jingcheng, Zhao Jinling. Diffenentiation of yellow rust and powdery mildew in winter wheat and retrieving of disease severity based on leaf level spectral analysis [J]. ***Spectroscopy and Spectral Analysis***, 2013, 33 (6): 1608-1614. (in Chinese)

[13] Huang Wenqian, Li Jiangbo, Zhang Chi. Identification of maize kernel embryo based on hyperspectral imaging technology and PCA [J]. ***Transactions of the Chinese Society of Agricultural Engineering***, 2012, 28(s2): 243-247. (in Chinese)

[14] Li Jiangbo, Rao Xiuqin, Ying Yenbing. Advance on application of hyperspectral imaging to nondestructive detection of agricultural products external quality [J]. ***Spectroscopy and Spectral Analysis***, 2011, 31(8): 2021-2026. (in Chinese)

[15] Ding L, Zhang Y P, Zhang X Y. Survey of image segmentation techniques and performance evaluation [J]. ***Computer Engineering and Software***, 2010, 31(12): 78-83.

[16] Wu Dewen, Zhang Yuanfei. The best density separation method for extracting rock information from remote sensing image [J]. ***Remote Sensing for Land & Resources***, 2002, 14 (4): 51-54. (in Chinese)

[17] Huang Changzhuan, Wang Bao, Yang Zhong. A Study on image segmentation techniques[J]. ***Computer Technology and Development***, 2009, 19(6): 76-79. (in Chinese)

[18] Feng Xinyue, Yang Qiuxiang, An Yanyan, et al. Research of image denoising based on support vector machine and wavelet coefficients [J]. ***Microelectronics & Computer***, 2014 (8): 119-122. (in Chinese)

[19] Zhang Jingcheng, Yuan Lin, Wang Jihua. Research progress of crop diseases and pests monitoring based on remote sensing [J]. ***Transactions of the Chinese Society of Agricultural Engineering***, 2012, 28 (20): 1 -11. (in Chinese)